Stability of Submarine Pipelines on Liquefied Seabeds

T. C. Teh[1]; A. C. Palmer[2]; M. D. Bolton[3]; and J. S. Damgaard[4]

Abstract: The conventional approach to pipeline stability design is reviewed and compared with experiments. A failure mechanism of pipelines on liquefied seabeds is analyzed. An analytical model to predict the pipelines sinking depth is proposed, and the comparison with measurements shows that the analysis is consistent with observed behavior.

DOI: 10.1061/(ASCE)0733-950X(2006)132:4(244)

CE Database subject headings: Submarine pipelines; Liquefaction; Sea floor; Waves; Geotechnical engineering.

Introduction

A marine pipeline is conventionally regarded to be stable if its weight generates enough lateral soil resistance to withstand the hydrodynamic force. The pipeline is idealized to be interacting with a stable seabed throughout its lifetime. This conventional approach has been set out in various codes and standards [e.g., BS 8010: Part 3, (British 1993); Veritec RP E305 (Veritas 1988)] and has also been described in a broad collection of books and papers (e.g., Bai 2001; Palmer and King 2004). As this is an established approach that has been accepted by the industry, and because there is extensive research literature on its details, most pipeline engineers assume that the conventional approach is reliable.

In reality, the seabed in shallow water usually becomes unstable before the extreme design conditions for the pipeline are reached. This fundamental flaw in the conventional approach to stability design was first pointed out by Palmer (1996). The issue has been pursued further within the EU LIMAS (Liquefaction around Marine Structures) program, which is conducted in collaboration between institutions in Denmark, France, Germany, the Netherlands, Norway, Poland, and the United Kingdom. Some preliminary results have been published (Damgaard and Palmer 2001; Teh et al. 2003; Palmer et al. 2004; Teh et al. 2004). The present paper first studies the performance of pipelines on liquefied beds in experiments by comparing the design results obtained from the conventional approach. It then proposes a failure mechanism of pipeline stability during seabed liquefaction and an analytical model of pipeline sinking depth. The results are compared with measurements on the pipeline model in wave flume experiments (Teh 2003; Teh et al. 2003).

[1]Pipeline Engineer, Intec Asia Pacific, 10th Floor, Menara Aik Hua, Changkat Raja Chulan, 50500 Kuala Lumpur, Malaysia.

[2]Research Professor, Univ. Engineering Dept., Univ. of Cambridge, Cambridge CB2 1PZ, U.K.

[3]Professor, Univ. Engineering Dept., Univ. of Cambridge, Cambridge CB2 1PZ, U.K.

[4]HR Wallingford Ltd., Howbery Park, Wallingford OX10 8BA, U.K.

Note. Discussion open until December 1, 2006. Separate discussions must be submitted for individual papers. To extend the closing date by one month, a written request must be filed with the ASCE Managing Editor. The manuscript for this paper was submitted for review and possible publication on May 7, 2004; approved on September 13, 2004. This paper is part of the ***Journal of Waterway, Port, Coastal, and Ocean Engineering***, Vol. 132, No. 4, July 1, 2006. ©ASCE, ISSN 0733-950X/2006/4-244–251/$25.00.

Conventional Approach to Stability Design

It is instructive to apply the conventional approach to stability design to examine the case studied in the experiments, described in detail elsewhere (Teh 2003; Teh et al. 2003).

In the wave flume the water was 0.45 m deep and the limestone silt bed 0.3 m deep. The silt had a specific gravity of solids of 2.71, d_{10}=0.010 mm and d_{50}=0.033 mm. The maximum and minimum voids ratios were 1.18 and 0.39, giving minimum and maximum bulk densities of 1,784 and 2,230 kg/m^3. Regular waves were generated at 1.25 s wave period with a wavelength of about 2.12 m. The wave height (crest to trough) was limited to 0.22 m to avoid breaking. The pipe diameter was 0.075 m.

In the conventional approach lateral resistance is modeled by a frictional model, so that the necessary submerged weight is determined from

$$F_H \leqslant \mu(w_p' - F_L) \tag{1}$$

where F_H=horizontal hydrodynamic force per unit length on the pipeline; F_L=lift force; w_p'=submerged weight of the pipeline; and μ=friction coefficient, here taken as 0.6. The hydrodynamic forces are generally estimated from Morison's equations described in Eqs. (2) and (3) (Sarpkaya and Isaacson 1981; Sumer and Fredsoe 1997)

$$F_H = \underbrace{\frac{1}{2}C_D\rho_w(u_w - u_p)|(u_w - u_p)|D}_{\text{Drag force}} + \underbrace{\frac{\pi}{4}\rho_w D^2(C_M - 1)\left(\frac{d(u_w - u_p)}{dt}\right)}_{\text{Added mass force}} + \underbrace{\frac{\pi}{4}\rho_w D^2\left(\frac{du_w}{dt}\right)}_{\text{Froude-Krylov force}} \tag{2}$$

$$F_L = \tfrac{1}{2}C_L\rho_w(u_w - u_p)^2 D \tag{3}$$

where C_D=drag force coefficient; C_M=inertia force coefficient; C_L=lift force coefficient; u_w=instantaneous velocity of water; u_p=instantaneous velocity of pipe; du_w/dt=instantaneous horizontal acceleration of water; D=pipe diameter; and ρ_w=water density. Following the Veritec RP E305 static analysis, u_p is taken as 0 m/s, C_D is 1.2, C_M is 3.29, and C_L is 0.9.

Combining Eqs. (1)–(3), the required mean specific gravity of the pipe s_p is

$$s_p = \frac{w_p}{(\pi D^2/4)\rho_w} = \frac{2}{\pi}\frac{C_D}{\mu}\frac{U_m^2}{gD}|\cos \omega t|\cos \omega t + 2\pi\frac{C_M}{\mathrm{KC}\mu}\frac{U_m^2}{gD}\sin \omega t + \frac{2}{\pi}C_L\frac{U_m^2}{gD}\cos^2 \omega t + 1 \quad (4)$$

where U_m=maximum fluid velocity; ω=wave angular frequency; t=time; g=gravity acceleration; and KC=Keulegan-Carpenter number defined as $U_m T/D$ (where T=wave period). On the right-hand side of Eq. (4), the first term is the normalized drag force, the second term is the normalized inertia force, the third term is the normalized lift force, and the fourth term is the normalized buoyancy force. With the parameters stated above, the maximum value of s_p is 1.46, reached when ωt is $\pi/2$. Accordingly, if the pipe were designed with that specific gravity it would be expected to be stable.

In the experiments, the pipe and the seabed behaved differently. When KC exceeded 1, the bed liquefied. At larger values of KC the pipe moved both vertically and horizontally. At the highest value of KC, 3.1, the horizontal back-and-forth movement of the pipe was about 0.4 diameters (Teh et al. 2003, Fig. 17) and the pipe sank until it was about three-quarters buried. This confirms that the conventional approach is relevant for a pipeline before the bed becomes unstable, but not for a pipeline after liquefaction occurs.

Liquefaction and Shearing around a Pipeline

Seabed liquefaction is complicated and not fully understood. It is thought that the liquefaction problem engages with both soil mechanics and sediment transport, and both specialists use different languages to communicate. The recent results of liquefaction experiments due to earthquakes (Butterfield and Bolton 2003) and waves (Teh et al. 2003; Palmer et al. 2004; Teh et al. 2004) have shown that the conventional interpretation that the seabed liquefaction must happen in an undrained condition and that the soil density remains constant is difficult to justify. Under the cyclic loading, it is observed the lower soil layer compacts to release water and the upper layer becomes dilated and looser.

A loose sand or silt seabed may consist of relatively recent sediment, which may be vulnerable to residual excess pore pressure liquefaction induced by a long return-period storm. After many storm waves followed by seabed settlement and densification, it may become very dense with relative density of about 100%. However, we still do not know whether a storm can loosen a bed under certain circumstances so that the relative density decreases as a result of the storm. A dense bed can still be eroded into sheet flow or plug flow if the storm-induced shear force is large enough to induce shear failure (Sleath 1994; Zala Flores and Sleath 1998; Sleath 1999) but that will only affect a layer that will normally be at least one order of magnitude smaller than a typical pipe diameter.

In the case of severe wave conditions that cause a seabed to become unstable, new considerations should be taken into account in stability design. During liquefaction, intense shear deformation of the soil can occur around pipelines. If the voids ratio is at the critical state, the soil continues to deform without any change in volume; if the voids ratio is less than the critical void ratio, the soil dilates under shear; if the voids ratio is more than the critical void ratio, the soil contracts.

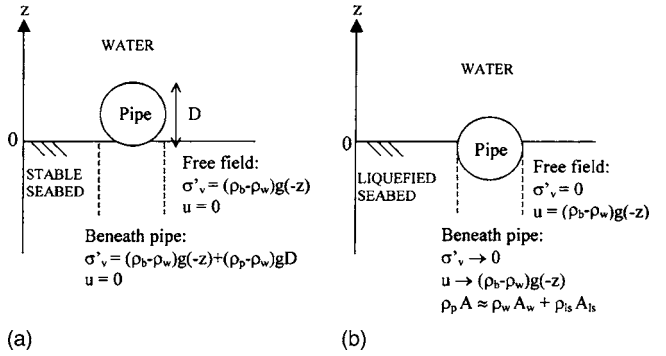

Fig. 1. Effective stress of soil and excess pore pressure at free field and beneath a pipe (a) before liquefaction; (b) during liquefaction

Most seabeds may have a relative density D_r of the order of 35% after deposition of suspended sediments, or a higher relative density after wave compaction, as implied from the present wave flume experiment. Since the relative density at the critical state is near the loosest state (D_r=0%) at low effective stress, the bed will always be denser than the critical state. This suggests that soils around pipelines will dilate to a critical state when they are sheared. The dilation of soil particles in the shear zone increases the void space between particles. Unless the pore water is compressible or cavitates, additional pore fluid has to feed into the increased void space from the surrounding soil. The inward flow requires a pore pressure gradient that may depend on speed of pipe movement and types of shearing.

Palmer (1999) explains the speed effect in cutting and ploughing, and those ideas may also apply to pipe penetration through a saturated soil. If the pipe sinks slowly, the pore pressure changes are small because only a small pressure gradient is needed to drive the slow flow of pore water; if the pipe sinks faster and the soil is dilatant, the pore pressure drops substantially in the heavily deformed region in order to generate a large enough pressure gradient to drive the flow rapidly. This pore pressure response around the pipe may be different from the undrained behavior of a saturated and cyclically loaded soil. Under cyclic loading, suction of pore fluid may occur around a marine structure but plenty of water will be fed into the shear zone rapidly from a water source zone. The excess pore pressure will increase towards the value that corresponds to the submerged weight multiplied by the depth from the surface.

Fig. 1 describes schematically the effective stress transmitted by soil particles and excess pore pressure before and during liquefaction: σ_v' denotes the effective stress; u=excess pore pressure; ρ_b=bulk density of soil; ρ_{ls}=bulk density of liquefied soil; ρ_w=density of water; ρ_p=average density of pipe; g=gravity acceleration; D=pipe diameter; A=pipe area; A_w=pipe area exposed water; and A_{ls}=pipe area exposed to liquefied soil. Before liquefaction, the effective stress transmitted by soil particles at the free field equates to the submerged weight of soil multiplied by the depth, since no excess pore pressure is present. The effective stress beneath a pipe is higher due to the additional submerged weight of the pipe. During liquefaction, the excess pore pressure in the free field increases to a value of submerged soil weight multiplied by the depth, which in turn reduces the effective stress to zero. Since the density of pipe is balanced by the density of water and liquefied soil around it, the effective stress below it is near zero, depending on the excess pore pressure, which may be slightly lower than the free field at the same level. A zero effec-

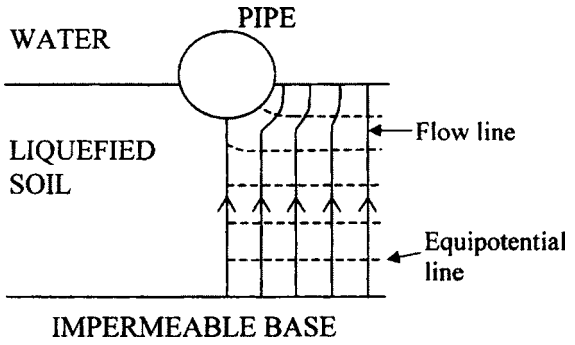

Fig. 2. Flow through a flow net

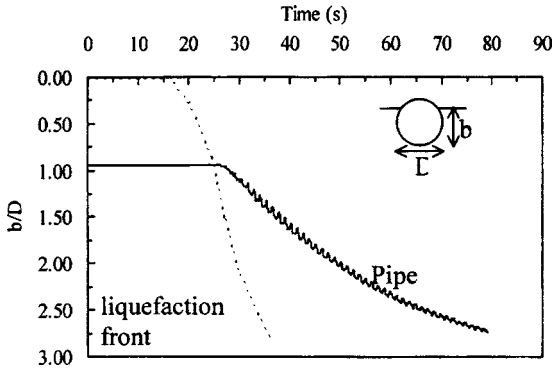

Fig. 3. Comparison between pipe displacement and liquefaction front advance in Test TM01

tive stress indicates that the soil has no stiffness or resistance to shear.

Fig. 2 shows the flow net at the instant where the excess pore pressure has built up before the occurrence of full liquefaction. It refers to the mean flow induced by the increase of pore pressure that precedes liquefaction, and excludes the dynamic changes at the wave frequency due to pore pressure changes at the mudline. The water has to flow from one "source" at the bottom of the soil bed into a "sink" at the top layer in the direction of the hydraulic gradient induced by the excess pore pressure. The flow lines are the trajectories of particles of water, and the equipotential lines are lines joining points in the soil that share the same excess pore pressure over a datum. The soil may start to liquefy around the pipe first because of the higher pressure gradient compared to a lower pressure gradient at free field. The flow may become unsteady after liquefaction occurs. The migrated water mixes with the soil particles in the vicinity of the pipe, which is further enhanced by the distortion due to the motion of the pipe itself and the wave-induced cyclic shear stress. The liquefied soil can rearrange to a critical voids ratio under the continuous shearing, and behaves like a heavy fluid. The increment of water content due to the transient flow of pore fluid softens the soil by reducing the soil undrained shear strength. The reduced stiffness of the liquefied soil causes the pipe to lose the lateral resistance to withstand the hydrodynamic force and base resistance to support its own weight.

Instability of Pipelines

The liquefaction phenomenon discussed in the preceding section is closely related to pipeline stability. Fig. 3, from the experiments of Teh (2003), shows the movement of a pipe that has started to sink after the bed in the free field has liquefied. The displacement of the pipe is measured by a linear position transducer. The position of the liquefaction front is computed from the excess pore pressure measured at about 0.6 m from the front of the pipe. The time lag between the measurements is about 30% of the wave period as the wavelength is 2.12 m. This is in contrast to Sumer et al.'s (1999) experimental observation that the pipe began to sink before excess pore pressure reached the overburden pressure at free field. Sumer et al. (2002) observed that the excess pore pressure built up more rapidly to the initial overburden pressure at the bottom of a fixed pipe than in the free field.

Fig. 4 compares the displacement of pipes with one degree of movement freedom for different pipe specific gravity s_p and test conditions. The displacement is described by the ratio b/D between the pipe embedment b and the pipe diameter D. The heavier pipe sank faster and to a greater depth. The sinking velocity seemed to be neither constant nor linear, which is in conflict to Sumer et al.'s (1999) observation that their buried pipe with initial $b/D=1.75$ sank with a constant velocity.

A heavy pipeline sinks into the liquefied soil, and a light pipe floats. Fig. 5 shows the initial position and final position of a wide range of pipe specific gravities for different degrees of freedom after liquefaction occurred. The initial and final depth from the pipe bottom to the surface layer is normalized with respect to pipe diameter. Two types of experiments were carried out: "one degree of movement freedom" refers to a pipe that is free to move vertically, but not free to rotate in plan or to move horizontally, whereas "two degree of movement freedom" refers to a pipe that can move horizontally as well as vertically.

A hypothesis is that the pipeline stops sinking in three different ways, depending on its specific gravity and the behavior of the liquefied soil. Firstly (Mode I), if a light pipe sinks slowly, the pressure gradient in pore fluid due to the excess pore pressure in the liquefied soil or the density of liquefied soil (heavy fluid) will

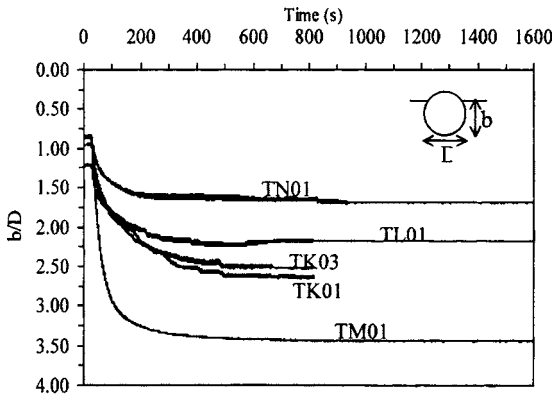

test	pipe specific gravity	initial b/D	wave height (m)	wave loading
TK01	1.90	1.2	0.15	0-800 s
TK03	1.91	1.2	0.22	0-750 s
TL01	1.88	0.84	0.20	0-820 s
TM01	1.99	0.94	0.20	0-800 s
TN01	1.82	0.86	0.19	0-950 s

Fig. 4. Time series of one degree of movement freedom pipe displacement

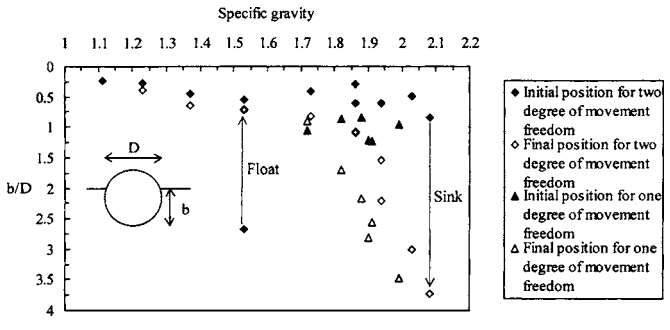

Fig. 5. Sinking/floatation depth of different pipe specific gravities

act as a buoyancy force to suspend the pipe. The pressure gradient increases with depth, in order to support the increasing density of liquefied soil with depth. Secondly (Mode II), if the excess pore pressure in liquefied soil dissipates rapidly before the pipe can reach an equilibrium pressure gradient or if the pressure gradient is not large enough, the pipe will stop sinking when it reaches the upwards propagating stable layer with higher shear strength. This is because the water content drops when the pore fluid drains into the layer above, which, in turn, increases the bearing capacity. Thirdly (Mode III), if a heavy pipe sinks fast enough before the dissipation of excess pore pressure, or if the pressure gradients are not sufficient to support the pipe, it will continue to sink until it reaches a nonliquefied and stable soil layer in elastic zone or impermeable base.

The sinking depth of a pipe on a liquefied seabed may be verified by using the experimental results shown in Fig. 6. The density of liquefied soil in the free field, which is labeled by open symbols, was assessed in three different ways: a pipe acting as a hydrometer which floats on a fully liquefied soil, a conductivity probe, and a local pressure gradient at two different depths. The equilibrium or ultimate depth that a heavy pipe sinks to during liquefaction is labeled by closed symbols, plotted at the center of each pipe, with a vertical line passing through the solid symbols representing the pipe diameter. The average density of the pipe was determined from its known weight and volume.

Pipes with two degrees of movement freedom end up within the liquefied region (Mode I). Their weights are balanced by a pressure gradient around the pipe, in which the hydrostatic pressure gradient of liquefied soil $\rho_{ls}g$ causes the pipe to feel a positive buoyancy force. However, pipes with one degree of freedom are observed to sink more than the pipes with two degrees of

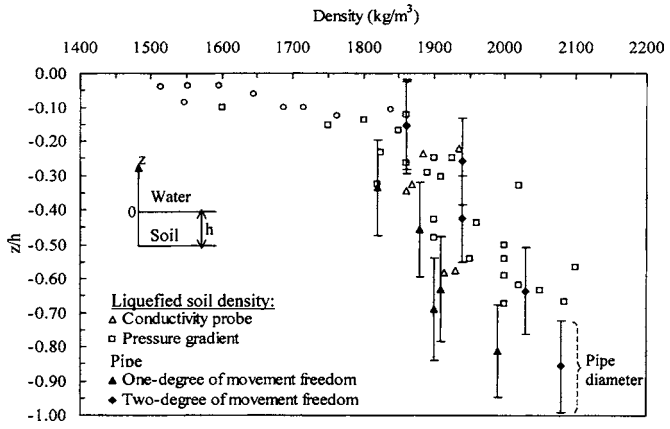

Fig. 6. Equilibrium depths of pipes with different densities

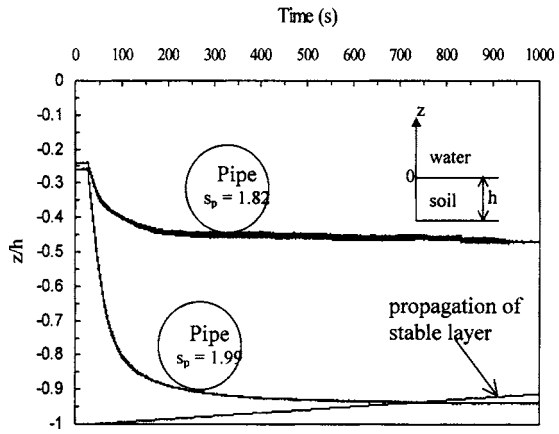

Fig. 7. Displacement of pipes and upward propagation of stable layer

freedom. This suggests that the additional cyclic horizontal movement of a pipe may create a cyclic loading effect to shear the soil around it to a state of full liquefaction, a form of the same phenomena as the wave-induced cyclic loading to shear the soil at free field. If horizontal movement is prevented without the additional cyclic loading (horizontal cyclic movement) from the pipe itself, the soil may not be fully sheared around the pipe, and then the local excess pore pressure is lower.

The Mode II of sinking can be better interpreted in Fig. 7. The propagation of a stable layer starting from the deepest soil layer is determined by a proposed analytical solution described in the Appendix. Fig. 7 shows that a pipe with specific gravity of 1.82 stops sinking much earlier than a pipe with specific gravity of 1.99. This is because the lighter pipe is light enough to be suspended by the pressure gradient around it as explained earlier as Mode I. A heavier pipe may be heavy enough to penetrate through the liquefied soil until it hits a stable layer that propagates upwards from the permeable base of the flume.

A pipe with a specific gravity of 2.08 sinks to the impermeable base of the flume. The pressure gradient or the density of liquefied soil is not large enough to suspend the heavy pipe, and the upper boundary of the stable layer has not traveled upwards fast enough.

The distance to which pipes sink in Modes II and III must depend in part on the gradation of density with depth within the mobile layer, and this is being investigated separately.

Design Implications

The main task for a pipeline designer considering the possible relevance of the conventional approach during storm conditions will be the susceptibility of the seabed to liquefaction. If the seabed is stable, the conventional approach is adequate; but if the seabed can become unstable, an alternative approach should be developed and adopted to account for the seabed mobilization. It is difficult to follow the conventional guidelines to prevent the horizontal movement of a pipe, unless it is designed as a very heavy pipe (e.g., specific gravity more than 2) or anchored at very short intervals (e.g., less than 20 m) so that it is rigid. These measures are not practical because the cost of construction would be high.

The mobile layer thickness is a concern because it determines the pipe behavior. If the soil around the pipe becomes liquefied, a more efficient way to design the pipe stability may be to control the horizontal movement through the self-burial of a pipe. A mini-

mum specific gravity is required so that the pipeline will become self-buried to a preferred pipe embedment when the bed becomes unstable or liquefied. The required specific gravity can be determined from the equilibrium of vertical forces acting on a pipe, which is described in the next section.

Analytical Model

This paper makes no distinction between liquefied soil and mobile soil. The pipe with weight w_p per unit length is in equilibrium with the buoyancy force per unit length F_B, the wave-induced lift force per unit length F_L, and the bearing capacity from liquefied soil, which follows:

$$w_p = F_B + F_L + NS_uD \tag{5}$$

where N=bearing capacity factor; S_u=undrained shear strength; and D=pipe diameter. The pipe weight per unit length w_p can be expressed as

$$w_p = s_p\rho_w gA \tag{6}$$

where s_p=pipe specific gravity; ρ_w=water density; g=gravity acceleration; and A=pipe area.

Eq. (5) is a general equation for equilibrium force, which applies to an on-bottom pipe on either nonliquefied soil or liquefied soil, and to a buried pipe in a liquefied soil. If the pipe is light ($w_p < F_B+F_L+NS_uD$), the pipe floats up so that the buoyancy force and bearing capacity decrease until they satisfy Eq. (5); if the pipe is heavy ($w_p > F_B+F_L+NS_uD$), the pipe sinks so that the buoyancy force and bearing capacity increase until they satisfy Eq. (5).

The buoyancy force F_B per unit length is the effect of pressure gradient of water $\rho_w g$ and pressure gradient of liquefied soil $\rho_{ls}g$, which follows Eq. (7). The term $\rho_{ls}g$ is described in the Appendix

$$F_B = \rho_w gA_w + \rho_{ls}gA_{ls} \tag{7}$$

where A_w=pipe area submerged in the water; A_{ls}=pipe area submerged in the liquefied soil; ρ_w=water density; ρ_{ls}=liquefied soil density (which might correspond to the critical void ratio of soil); and g=gravity acceleration. A_{ls} can be computed from Eq. (8) and A_w can be obtained from the difference between A and A_{ls}

$$A_{ls} = \frac{\psi D^2}{8} - \left(\frac{D^2}{4} - \frac{bD}{2}\right)\sin\frac{\psi}{2} \tag{8}$$

where $\psi = 2\arccos(1-2b/D)$; and b=pipe embedment in a liquefied soil.

The lift force per unit length F_L is a hydrodynamic force generated by the pressure difference around a pipeline, and is determined from Morison's equations (Morison et al. 1950)

$$F_L = \tfrac{1}{2}C_L\rho_w(u_p - u_w)^2D \tag{9}$$

where C_L=lift force coefficient; u_p=pipe velocity; u_w=water velocity; and D=pipe diameter. C_L falls with increasing embedment of the pipe. It also depends on the Reynolds number U_mD/ν or Keulegan-Carpenter U_mT/D number and the pipe surface roughness where U_m=maximum velocity of water; ν=kinematic viscosity; and T=wave period.

If the seabed becomes liquefied when its effective stress is about zero, its bearing capacity may be negligible. In such the case, a floating pipe embedment b in the liquefied soil or specific gravity s_p can be determined using Eq. (10) that is derived from Eq. (5), but in a different form

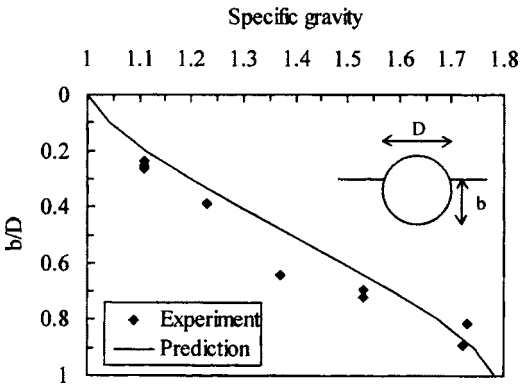

Fig. 8. Comparison between experimental observation and theoretical prediction for the embedment of floating pipe on liquefied soil at different pipe specific gravity

$$s_p = 1 + \left[\frac{\psi}{2\pi} + \left(\frac{2b}{\pi D} - \frac{1}{\pi}\right)\sin\frac{\psi}{2}\right]\left[\frac{\rho_{ls}}{\rho_w} - 1\right] + \frac{2}{\pi}C_L\frac{(u_p - u_w)^2}{gD} \tag{10}$$

where the density of liquefied soil ρ_{ls} may correspond to the critical void ratio of soil e_{crit} as described in, "Liquefaction and shearing around a pipeline" and can be expressed as

$$\rho_{ls} = \rho_w\left(\frac{G_s + e_{crit}}{1 + e_{crit}}\right) \tag{11}$$

Eq. (10) reduces to Eq. (12) when the lift force acting on the pipe is small and negligible

$$s_p = 1 + \left[\frac{\psi}{2\pi} + \left(\frac{2b}{\pi D} - \frac{1}{\pi}\right)\sin\frac{\psi}{2}\right]\left[\frac{\rho_{ls}}{\rho_w} - 1\right] \tag{12}$$

Eqs. (10) and (12) only apply when the embedment ratio b/D is less than 1. If b/D is greater than 1, the pipeline sinks until its specific gravity matches that of the surrounding soil.

This study has not attempted to quantify the details of the process of pore pressure buildup as liquefaction takes place, or to take account of local variations of pore pressure around the pipe. Mei and Foda (1981) applied a poroelastic model, but our experiments suggest that as movement begins any elastic model is unlikely to be a good idealization. Sumer et al. (1999) noted that the pipe begins to sink before the pore pressure reaches the overburden pressure, and argue that this happens partly because of the reduction in the soil strength caused by high pore pressures, and partly due to additional pore pressures close to the pipe. That explanation is entirely reasonable: indeed, the pipe must impose additional shear stresses on the soil (unless the pipe mean density precisely matches the mean density of the soil it displaces), and local deformation must begin before the pore pressure balances the overburden pressure.

Comparison with Measurements

Fig. 8 compares the experimental results with a prediction using Eq. (12), which was used because the wave-induced lift force and undrained shear strength of liquefied soil in the experiment were negligibly small (Teh et al. 2004). The voids ratio in the critical state at low effective stress is not immediately determined by any standard soil tests. It is therefore assumed that the liquefied soil is

at critical state and about zero effective stress, and that its density approximately corresponds to the maximum void ratio of the soil.

The agreement in Fig. 8 is good, although the prediction line is slightly higher than the experimental data points at lower pipe specific gravity. This is because the voids ratio in the top layer near the bed surface is higher than the assumed maximum void ratio. Since it is not yet practicable to predict the exact void ratio of liquefied soil, the nominal maximum void ratio e_{max} can be used to determine the required specific gravity for a pipe to self-bury into the liquefied soil at a preferred pipe embedment.

Discussion

It is useful to pause to reflect about what the pipeline operator and designer should expect from the design. In the past they have usually thought of "stability" as a requirement that the pipeline does not move at all, though sometimes that has been extended to accept limited horizontal movements. The Veritec recommended practice (RP) *E305* clause 4.2.3 allows a maximum lateral displacement of 20 m in a seastate duration of 3 h at maximum intensity, in zone 1 more than 500 m from a platform or template, "if no further information is available." It is not clear if repeated movement is allowable. The source of the 20 m figure is not stated, and the RP says that it can be relaxed "if other relevant data are available." Zone 2 is within 500 m of a platform, and there movement can be allowed "if the…displacement can be acceptably accommodated." The RP is shortly to be revised.

Movement as such has little or no effect on the operation of a pipeline, but it can lead to a limit state in which the structural security of the pipeline is compromised, either by excessive bending or by overloading of attached structures such as pipelines or wellheads. Limited downward vertical movement is not harmful, and may indeed often be beneficial, since it moves the pipeline to a level at which it is more secure against exposure by subsequent sediment transport, and less at risk from anchors and fishing gear.

It is tentatively proposed that the definition of stability should be extended to recognize the possibility of limited vertical and horizontal movement. The limits of movement depend strongly on the pipeline and the environmental conditions, and are outside the scope of the present paper.

The experiments were necessarily on a small scale, and it has not yet been possible to repeat the experiments on the larger scale of most marine pipelines in practice. Similarity issues need to be explored in more detail: but it appears that the key parameters are pipeline density, Sleath number, pipeline Sleath number (Damgaard and Palmer 2001), and wave steepness.

Conclusion

The conventional approach is used to design a pipe in the wave flume experiment so that the design result can be compared directly with the experimental results. Experimental results show that the conventional stationary-soil models of lateral resistance become irrelevant during severe wave conditions where the bed becomes liquefied. The approach always leads to a satisfactory result because it always ensures that the pipe is always heavy enough to sink faster into a mobile bed than it can be carried away.

Shear deformation due to the wave-induced or pipe-induced cyclic loading occurs around the pipe. This leads to the migration of water towards the pipe and soil softening. During seabed liquefaction (mobilization), an on-bottom pipe sinks until it reaches an equilibrium depth. Three possible ways are identified to stop the pipe from sinking: (1) the pressure gradient of excess pore pressure or density of liquefied soil around the pipe; (2) the stable layer that propagates upwards; and (3) the impermeable base or nonliquefied soil. They are verified with experimental results and also with a proposed analytical solution for the propagation velocity of a stable layer.

A new more rational stability design method is proposed. The pipe is assumed to be on an unstable seabed during storm conditions. In this alternative approach, the pipe is designed so that it becomes self-buried until a minimum pipe embedment during seabed liquefaction. An analytical solution is suggested where it predicts the pipe embedment with specific gravity of pipes. This solution assumes the density of liquefied soil to be in critical state, which may correspond to the maximum void ratio at very low effective stress. To generalize the finding, other sediments ought to be investigated in the future.

Comparing the conventional approach and alternative approach, the conventional approach may underdesign or overdesign the pipe specific gravity depending on the preferred pipe embedment during seabed liquefaction.

Acknowledgments

The experiments were carried out at HR Wallingford, and partially funded by the Commission of the European Union Directorate General XII within the Fifth Framework Programme with specific programme: "Energy, Environment and Sustainable Development" under Contract No. EVK3-CT-2000-00038, Liquefaction Around Marine Structures (LIMAS). T.C. Teh is partially supported by the Cambridge Commonwealth Trust, and Andrew Palmer by the Jafar Foundation. The writers are grateful for this support. The writers thank three reviewers for valuable comments.

Appendix: Computation for Upward Propagating Stable Layer

The stable layer propagates upwards with a velocity dL_c/dt where dL_c is a change of the length or thickness of the stable layer within the time duration of dt. The saturated soil with initial voids ratio e_0 in this layer densifies by a change of voids ratio Δe. The net outflow of water to unit volume of soil may therefore be written as Eq. (13)

$$v_c = \frac{dL_c}{dt}\frac{\Delta e}{(1+e_0)} \tag{13}$$

According to Darcy's law, the flow velocity is proportional to the permeability and pressure gradient (hydraulic gradient). In the case of soil liquefaction, the hydraulic gradient is taken as the critical hydraulic gradient i_{crit}, and therefore the Darcy velocity can be expressed by

$$v_{Darcy} = ki_{crit} \tag{14}$$

where $i_{crit}=(\rho_{ls}-\rho_w)/\rho_w$; k=soil permeability; and ρ_{ls} and ρ_w=density of liquefied soil and water, respectively.

As the dissipation of excess pore pressure obeys Darcy's law, the velocity of propagation of the stable layer may be written as Eq. (15), by equating Eq. (13) to Eq. (14).

$$\frac{dL_c}{dt} = k\frac{G_s - 1}{\Delta e} \tag{15}$$

where G_s=specific gravity of particles. It can be interpreted as the stable layer growing faster in a more permeable material or in a denser soil where the particles have little room to rearrange into a denser state. The height of the stable layer can be obtained by integrating Eq. (15) with time, so that

$$L_c = k\frac{G_s - 1}{\Delta e}t \tag{16}$$

Eq. (16) is used to plot the propagation of the stable layer in Fig. 8. The permeability may be correlated to the size of the sieve which just allows 10% by weight of the soil to pass d_{10} (Bolton 1979), which may be written as

$$k = 0.01(d_{10})^2 \tag{17}$$

in which the unit must be stated as m/s. d_{10} of the silt bed is found to be 10 μm, and therefore k is in the order of 10^{-6} m/s. G_s is found to be 2.71, and Δe is assumed to be in the order of 0.07 which is based on the difference of measurement between voids ratio during liquefaction at mid depth of soil and voids ratio after liquefaction at about 0.05 m from the bed surface.

Notation

The following symbols are used in this paper:

A = area of pipe;
A_{ls} = area of pipe submerged in liquefied soil;
A_w = area of pipe submerged in water;
b = pipe embedment;
C_D = drag force coefficient;
C_L = lift force coefficient;
C_M = inertia force coefficient;
D = pipe diameter;
D_r = relative density;
dL_c = change of the length or thickness of stable layer;
dL_c/dt = velocity of propagation of stable layer;
du_w/dt = instantaneous horizontal acceleration of water;
d_{10} = diameter at which 10% by mass of sample is smaller than this size;
d_{50} = diameter at which 50% by mass of sample is smaller than this size;
e = void ratio;
$e_{\max}$ = maximum void ratio;
e_0 = initial void ratio;
F_B = buoyancy force per unit length;
$F_{B\mathrm{ls}}$ = static buoyancy force per unit length of a body in liquefied soil;
F_{Bw} = static buoyancy force per unit length of a body in water;
F_H = total horizontal hydrodynamic force on a pipeline per unit length;
F_L = lift force per unit length;
$F_{L\mathrm{ls}}$ = lift force per unit length due to moving liquefied soil;
F_{Lw} = lift force per unit length due to moving water;
G_s = specific gravity of soil particle;
g = gravity acceleration;
i_{crit} = critical hydraulic gradient;
KC = Keulegan–Carpenter number ($=U_mT/D$);
k = soil permeability;
N = bearing capacity factor;
p_{mudline} = pressure at mudline;
S_u = undrained shear strength;
s_p = specific gravity of a pipe;
T = wave period;
t = time;
U_m = maximum velocity of water;
u = excess pore pressure;
u_p = instantaneous velocity of pipe;
u_w = instantaneous velocity of water;
v_c = net outflow of water;
v_{Darcy} = Darcy's flow velocity;
w_p = weight per unit length of a pipeline;
w_p' = submerged weight per unit length of a pipeline;
z = distance measured in the vertical direction upwards from the seabed surface;
Δe = change of void ratio;
μ = friction coefficient;
ν = kinematic viscosity;
ρ_b = bulk density of soil;
ρ_{ls} = bulk density of liquefied soil;
ρ_p = average density of pipe;
ρ_w = density of water;
σ_v' = initial effective stress;
ψ = $2\arccos(1-2b/D)$; and
ω = wave angular frequency ($=2\pi/T$).

References

Bai, Y. (2001). *Pipelines and risers*, Elsevier Science, Amsterdam, The Netherlands.

Bolton, M. D. (1979). *A guide to soil mechanics*, Macmillan, London.

British Standards Institution. (1993). "Code of practice for pipelines, Part 3, Pipelines subsea: Design, construction and installation." *BS 8010*, London.

Butterfield, K., and Bolton, M. D. (2003). "Modelling pore fluid migration in layered, liquefied soils." *Pacific Conf. on Earthquake Engineering*, Christchurch, New Zealand.

Damgaard, J. S., and Palmer, A. C. (2001). "Pipeline stability on a mobile and liquefied seabed: A discussion of magnitudes and engineering implications." *20th Int. Conf. on Offshore Mechanics and Artic Engineering*, Rio de Janeiro, Brazil.

Mei, C. C., and Foda, M. A. (1981). "Wave-induced stresses around a pipe laid on a poro-elastic sea bed." *Geotechnique*, 31, 509–517.

Morison, J. R., O'Brien, M. P., Johnson, J. W., and Schaaf, S. A. (1950). "The forces exerted by surface waves on piles." *J. Petrol. Technol., Petrol. Trans.*, 189, 149–154.

Palmer, A. C. (1996). "A flaw in the conventional approach to stability design of pipelines." *Proc., Offshore Pipeline Technology Conf.*, Amsterdam, The Netherlands.

Palmer, A. C. (1999). "Speed effects in cutting and ploughing." *Geotechnique*, 49(3), 285–294.

Palmer, A. C., and King, R. A. (2004). *Subsea pipeline engineering*, Pennwell, Tulsa, Okla.

Palmer, A. C., Teh, T. C., Bolton, M. D., and Damgaard, J. S. (2004). "Stable pipelines on unstable seabed: Progress towards a rational design method." *Proc., Offshore Pipeline Technology Conf.*, Amsterdam, The Netherlands.

Sarpkaya, T., and Isaacson, M. (1981). *Mechanics of wave forces on offshore structures*, Van Nostrand Reinhold, New York.

Sleath, J. F. A. (1994). "Sediment transport in oscillatory flow." *Sediment transport mechanisms in coastal environments and rivers*,

M. Belorgey, R. D. Rajaona, and J. F. A. Sleath, Eds., World Scientific, Singapore.

Sleath, J. F. A. (1999). "Conditions for plug formation in oscillatory flow." *Cont. Shelf Res.*, 19, 1643–1664.

Sumer, B. M., and Fredsoe, J. (1997). *Hydrodynamics around cylindrical structures*, World Scientific, Singapore.

Sumer, B. M., Fredsoe, J., Christensen, S., and Lind, M. T. (1999). "Sinking/floatation of pipelines and other objects in liquefied soil under waves." *Coastal Eng.*, 38, 53–90.

Sumer, B. M., Fredsoe, J., and Truelsen, C. (2002). "Liquefaction around a buried pipeline in progressive wave." *Workshop on Wave- and Seismic-Induced Liquefaction and its Implications for Marine Structures*, Istanbul, 14 and 15.

Teh, T. C. (2003). "Stability of marine pipelines on unstable and liquefied seabed." Ph.D. dissertation, Department of Engineering, Univ. of Cambridge.

Teh, T. C., Palmer, A. C., and Bolton, M. D. (2004). "Wave-induced liquefaction and the stability of marine pipelines." *Proc., Int. Conf. on Cyclic Behaviour of Soils and Liquefaction Phenomena, RuhrUniversität Bochum*, AA Balkema, Leiden, The Netherlands, 449–453.

Teh, T. C., Palmer, A. C., and Damgaard, J. S. (2003). "Experimental study of marine pipelines on unstable and liquefied seabed." *Coastal Eng.*, 50, 1–17.

Veritas. (1988). "On-bottom stability design of marine pipelines." *Veritec RP E305*, Veritas Offshore Technology and Services A/S, Hovik, Norway.

Zara Flores, N., and Sleath, J. F. A. (1998). "Mobile layer in oscillatory sheet flow." *J. Geophys. Res., [Oceans]*, 103(C6), 12783–12793.